2021 43rd Annual International Conference of the
IEEE Engineering in Medicine & Biology Society (EMBC)
Oct 31 - Nov 4, 2021. Virtual Conference

Muscle Activity Estimation at Drop Vertical Jump Landing Using Passive Muscle Mechanical Model

Hinako Suzuki[1], Akihiko Murai[2,3], Yosuke Ikegami[4], Emiko Uchiyama[5], Ko Yamamoto[4,6], Ayaka Yamada[4], Yuri Mizutani[6], Kohei Kawaguchi[6,7], Shuji Taketomi[6,7] and Yoshihiko Nakamura[6,8]

***Abstract*— Among the various elements that facilitate the movement of the lower limbs, the anterior cruciate ligament (ACL) is prone to injury. An adequate joint control of the lower limb can prevent ACL injury. Balancing activities between the agonist and the antagonist muscles is vital for joint control. However, prior studies on muscle activities were limited since they could not determine passive muscle activities. In this study, we develop a muscle model considering the passive properties to analyze the movement mechanism of the ACL under heavy loads, such as those produced during jump landing. We estimated the muscle activities occurring during a drop vertical jump (DVJ) by applying to the proposed method the physiological constraint that muscle activities are constant during a short time around landing. In addition, the knee joint torque and muscle forces were calculated from the estimated muscle activities, which were thereafter compared with those obtained using the conventional method. The results revealed that this passive muscle model appropriately represented the knee joint torque at DVJ landing by decreasing the passive muscle strain and increasing the isometric maximum muscle force. Moreover, the estimated muscle activities were larger than those obtained using the conventional method, which may be caused by the co-contraction between agonist and antagonist muscles that cannot be represented by the conventional method. This muscle co-contraction estimation algorithm would estimate the muscle load under heavy loads, and applying this knowledge to training would help to prevent ACL injuries.**

[1]Hinako Suzuki is with The Graduate school of Frontier Sciences, The University of Tokyo, 6-2-3 Kashiwanoha, Kashiwa, Chiba, 277-0882, Japan. suzuki.h1230@aist.go.jp

[2]Akihiko Murai is with Human Augmentation Research Center, National Institute of Advanced Industrial Science and Technology, 6-2-3 Kashiwanoha, Kashiwa, Chiba, 277-0882, Japan. a.murai@aist.go.jp

[3]Akihiko Murai is with Japan Science and Technology Agency, PRESTO, Kawaguchi, Saitama, japan. a.murai@aist.go.jp

[4]Yosuke Ikegami, Ko Yamamoto and Ayaka Yamada are with The Graduate school of Information Science and Technology, The University of Tokyo, 7-3-1 Hongo, Bunkyo-ku, Tokyo, 113-8656, Japan. {ikegami, yamamoto.ko, a_yamada}@ynl.t.u-tokyo.ac.jp

[5]Emiko Uchiyama is with Department of Mechanical Engineering, School of Engineering, Tokyo Institute of Technology, 2-12-1 Ookayama, Meguro-ku, Tokyo, 152-8552, Japan. uchiyama.e.aa@m.titech.ac.jp

[6]Ko Yamamoto, Yuri Mizutani, Kohei Kawaguchi, Shuji Taketomi and Yoshihiko Nakamura are with The University of Tokyo Sports Science Initiative, The University of Tokyo, 7-3-1 Hongo, Bunkyo-ku, Tokyo, 113-8656, Japan. yamamoto@ynl.t.u-tokyo.ac.jp, mizutanakayuri@gmail.com, kkohei0602@yahoo.co.jp, takeos-tky@umin.ac.jp, nakamura@race.t.u-tokyo.ac.jp

[7]Kohei Kawaguchi and Shuji Taketomi are with The Department of Orthopaedic Surgery, Faculty of Medicine, The University of Tokyo, 7-3-1 Hongo, Bunkyo-ku, Tokyo, 113-8655, Japan. kkohei0602@yahoo.co.jp, takeos-tky@umin.ac.jp

[8]Yoshihiko Nakamura is with The Graduate school of Engineering, The University of Tokyo, 7-3-1 Hongo, Bunkyo-ku, Tokyo, 113-8656, Japan. nakamura@race.t.u-tokyo.ac.jp

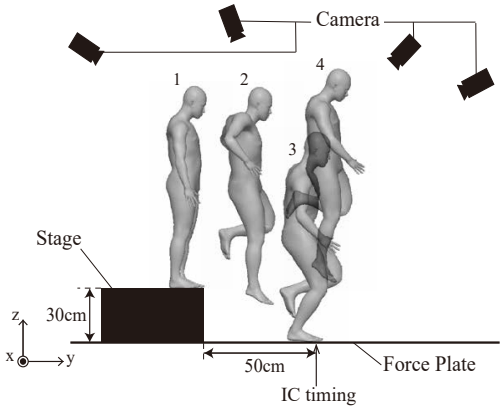

Fig. 1. Scheme of drop vertical jump (DVJ) measurement, where 24 cameras are used to capture the jump activity. The jump is performed from the stage to the ground. In addition, two force plates are placed on the ground to measure the contact force against the floor. A line is drawn 50 cm away from the edge of the stage. The participant was asked to jump toward the line 50 cm away from the 30-cm-high stage and to jump as high as possible soon after landing on the ground. The initial contact (IC) denotes the timing of landing on the line.

I. Introduction

Injuries, especially in the lower limbs, occur frequently in sports that involve vigorous physical activity. Among the various elements that facilitate lower limb movement, the anterior cruciate ligament (ACL), which connects the femur and the tibia and stabilizes the knee joint, is one of the most frequently injured structures during high impact or sporting activities. Due to the poor capacity of the ACL to heal, patients with torn ACLs often require surgery. The healing process after the surgery is quite long, i.e., six months or more, which is the time taken before returning to sports. Around 70% of ACL injuries are noncontact-type injuries that are caused by large loads applied on the knee without contact with other persons, such as jump landing or sudden stop in movement or change in direction [1]. Therefore, the incidence of ACL injury can be significantly reduced by preventing noncontact-type injuries. The position control error of lower limb joints, such as excessive knee valgus in a dynamic state, can result in a noncontact ACL injury [2][3]. Thus, an adequate joint control would prevent ACL injury. From observations of jumps of participants, we noticed that their knee bending patterns at landing exhibited a typical characteristic. Some landed softly with a large bending, whereas others landed stiffly with a small bending. Whole-body balance control is another important characteristic;

however, we do not focus on it in this study. Instead, we aim to find a parameter that characterizes the difference between soft and stiff landings. A balance of activities between the agonist and the antagonist muscles is vital for joint control in the cases in which the knee is subjected to large loads, such as when decelerating from high speeds [4]. The agonist muscle plays a pivotal role in conducting a particular movement, whereas the antagonist muscle acts in the direction opposite to the agonist muscle. The hypothesis is that athletes prepare for landing by setting the co-contraction of the antagonistic muscles for stiffness control. Subsequently, the issue is the identification of the level of co-contraction at landing. A prior study has estimated such muscle activities based on motion capture data [5]. The inverse kinematics and inverse dynamics of the three-dimensional joint positions obtained from the motion capture system were solved using mathematical optimization calculations to estimate the muscle forces. This method can be applied to actual sports using a video-based motion capture system. However, the antagonist muscle activity cannot be estimated through this method as the optimization is performed with an objective to minimize the square sum of muscle forces; in this case, the antagonist muscle activity would be equal to zero. On the contrary, an electromyogram (EMG) can directly measure the muscle activity with the aid of electrodes attached to the human body. Although the antagonist muscle activity can be estimated using EMGs, exercising with electrodes attached to the body is challenging for participants in actual sports.

In this light, the present study develops a co-contraction identification method and verifies it experimentally through motion/force measurements using optical motion capture and force plates. The idea is to assume that an athlete sets and retains the muscle activity to prepare for landing, namely, for a short period of time, including the instant of landing. The computed knee joint torques from inverse dynamics based on the motion capture data vary in time and by motion patterns, which are the results of the passive stiffness revealed from the level of co-contraction. Video-based studies of ACL injuries reported that noncontact ACL injuries occurred within 40 ms after landing [6], and the muscle stretch reflexes appeared approximately 60 ms after landing [7]. Therefore, posture control with muscle stretch reflex or voluntary muscle control is theoretically difficult to achieve in case of landing to noncontact ACL injury. As the posture is fixed and prepared for landing immediately before landing, in this study, we hypothesized that the muscle activities are constant in a short period of time before and after landing, and the variation in the muscle force is caused by a passive mechanism, that is, viscoelasticity of the muscle. Using this hypothesis, we developed a calculation method that could determine the distribution of muscle activity between agonist and antagonist muscles [8]. However, we did not consider the detailed muscle properties under large passive forces. This study investigated a passive muscle mechanical model that was suitable for environments having heavy loads such as jump landing by considering the passive properties of the muscle. We studied the drop vertical jump (DVJ) motion, which constitutes one of the screening tests for ACL injury [2] and which is depicted schematically in Fig. 1. The muscle activities occurring before and after landing were estimated using the developed muscle model that incorporated the passive muscle properties into the Hill's equation [9]. The passive muscle mechanical model was adjusted for suitability by varying the parameters for landing. Furthermore, we compared the estimated agonist and antagonist muscle activities with those obtained using the conventional method to demonstrate the possibility of estimating muscle co-contractions. The remainder of this paper is structured as follows: Section II introduces the setup and procedure of DVJ motion measurement. Section III describes the conventional method and the method proposed for the estimation of muscle activity. Section IV and V present the results and discussions, respectively. Lastly, Section VI presents the conclusion of this study.

II. DVJ MOTION MEASUREMENT

The setup and procedure of precise DVJ motion measurement using optical motion capture and force plates are described in this section. The obtained data were used to analyze the muscle activities. The measurement was performed as follows [12][13]: The participant was asked to jump toward a line 50 cm away from the 30-cm-high stage. Within a short period after landing on the ground, the participant was asked to jump as high as possible. Fig. 1 shows the measurement environment and DVJ motion. We performed the DVJ measurement of the right-foot-landing on one subject. The subject was a 29-year-old man who had 15 years of swimming and 2 years of triathlon experiences. The initial contact (IC) was defined as the instant at which the heel or toe first landed on the ground. Subsequently, the muscle activity of the right lower limb was analyzed at IC. The motion was measured using an optical motion capture system using 24 cameras at 200 Hz (Raptor-4S, Motion Analysis Co., Santa Rosa, USA). The subject wore 57 markers. In addition, the contact force between the subject and floor was measured at 1 kHz with two force plates (ITR, Bertec Co.). The subject was free of any injuries at the time of data collection. Our study protocol was approved by the local institutional review board and conformed to the guidelines outlined in the Declaration of Helsinki (1983), and the subject provided informed consent.

III. ALGORITHM FOR MUSCLE ACTIVITY ESTIMATION

A. Conventional muscle activity estimation method [5]

This subsection describes the conventional method for estimating the muscle activity based on the muscle force [5]. The inverse kinematics of the involved motion was computed to estimate the three-dimensional joint positions using the optical motion capture data, whereas the inverse dynamics was evaluated to estimate the joint torque $\boldsymbol{\tau}$ generated at the joint positions and the consequent contact force against the floor. The relationship between the muscle force $\boldsymbol{f}$ and $\boldsymbol{\tau}$ is

represented as follows:

$$\boldsymbol{J}_{\ell} = \frac{\partial \boldsymbol{\ell}}{\partial \boldsymbol{\theta}}. \tag{1}$$

$$\boldsymbol{\tau} = \boldsymbol{J}_{\ell}^{T} \boldsymbol{f}, \tag{2}$$

where $\partial \boldsymbol{\ell}$ denotes the variation in the muscle length; $\partial \boldsymbol{\theta}$, the variation in the joint angle; and $\boldsymbol{J}_{\ell}$, the Jacobian matrix representing the variation in the muscle length based on that of the joint angle. Moreover, the following mathematical optimization minimizing the least-squares sum of muscle forces was solved to uniquely determine the muscle force, as humans operate on a redundant drive system in which the number of muscles is much greater than that of joints.

$$\arg\min_{\boldsymbol{f}} \frac{1}{2} \boldsymbol{\delta}_{\boldsymbol{\tau}}^{T} \boldsymbol{W}_{\boldsymbol{\tau}} \boldsymbol{\delta}_{\boldsymbol{\tau}} + \frac{1}{2} \boldsymbol{\delta}_{\boldsymbol{f}}^{T} \boldsymbol{W}_{\boldsymbol{f}} \boldsymbol{\delta}_{\boldsymbol{f}} \tag{3}$$

$$\boldsymbol{\delta}_{\boldsymbol{\tau}} = \boldsymbol{\tau} - \boldsymbol{J}_{\ell}^{T} \boldsymbol{f} \tag{4}$$

$$\boldsymbol{\delta}_{\boldsymbol{f}} = \boldsymbol{f} - \boldsymbol{f}^{*} \tag{5}$$

where $\boldsymbol{W}_{\boldsymbol{\tau}}$ and $\boldsymbol{W}_{\boldsymbol{f}}$ represent the weights of each evaluation term, and $\boldsymbol{f}^{*}$ denotes the muscle force measured by the EMG (it is 0 for unused muscles). As expressed in the second term of Eq. (3), the antagonist muscle activity in which the EMG was not attached would be equal to zero because the optimization calculation was solved to minimize the sum of squares of muscle forces.

B. Estimation method for antagonist muscle activity using Hill–Stroeve model and passive properties of muscle

This subsection describes the algorithm used in this study to develop the passive muscle mechanical model. The model was used to estimate the antagonist muscle activity under large passive forces such as jump landing. The passive properties of the muscles, which were not considered in [8], were applied to the developed model for analysis.

τ was estimated using the optical motion capture data in the same manner as the conventional method described in the subsection III-A. We used Hill–Stroeve ' s musculo-tendon model that represents the passive properties of muscles in detail. The relationship between the muscle activation $\boldsymbol{a}$ and $\boldsymbol{f}$ was represented as Eq. (6) by Hill [9]:

$$\boldsymbol{f} = \boldsymbol{F}_{max} \boldsymbol{F}_{lce}(\boldsymbol{\ell}) \boldsymbol{F}_{vce}(\dot{\boldsymbol{\ell}}) \boldsymbol{a}, \tag{6}$$

where $\boldsymbol{\ell}$ is the muscle length; $\dot{\boldsymbol{\ell}}$, the muscle velocity; and $\boldsymbol{F}_{max}$, the maximum isometric force. Stroeve [10] and Thelen [11] identified the force–length relationship $F_{lce}(\ell)$ and the force–velocity relationship $F_{vce}(\dot{\ell})$ as follows:

$$F_{lce}(\ell) = \mathrm{e}^{-(\ell/\ell_0 - 1)^2/\gamma} + \frac{\mathrm{e}^{k^{PE}(\ell/\ell_0 - 1)/\varepsilon_0^M} - 1}{\mathrm{e}^{k^{PE}} - 1} \tag{7}$$

$$F_{vce}(\dot{\ell}) = \begin{cases} 0 & (\dot{\ell} < -v_{max}) \\ \frac{V_{sh}(v_{max} + \dot{\ell})}{V_{sh} v_{max} - \dot{\ell}} & (-v_{max} \le \dot{\ell} < 0) \\ \frac{V_{sh} V_{shl} v_{max} + V_{ml} \dot{\ell}}{V_{sh} V_{shl} v_{max} + \dot{\ell}} & (\dot{\ell} \ge 0) \end{cases} \tag{8}$$

$$\ell_0 = \ell_{min} + L_{opt}(\ell_{max} - \ell_{min}) - \ell_t \tag{9}$$

$$\ell_{sh} = L_{sh}(\ell_{max} - \ell_{min}) \tag{10}$$

$$v_{max}(a, \ell) = V_{vm}(1 - V_{er}(1 - a F_{lce}(\ell))), \tag{11}$$

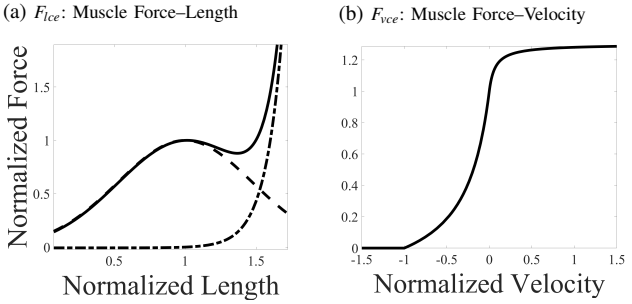

Fig. 2. Muscle force–length and force–velocity relationship.

where ℓ_0 denotes the original length; γ, the width of the Gaussian force–length curve; k^{PE}, the exponential shape factor; ε_0^M, the passive muscle strain resulting from the maximum isometric force; v_{max}, the maximum contraction velocity; V_{ml}, the maximum velocity during concentric contraction; L_{opt}, the relative optimum muscle length; ℓ_t, the tendon length; and L_{sh}, the relative width of the force–length curve. Further, V_{sh}, V_{shl}, V_{vm}, and V_{er} are parameters for the force–length curve, and ℓ_{min} and ℓ_{max} are the minimum and maximum muscle length, respectively. The first and second terms of Eq. (7) represent the active and passive properties of the muscle, respectively. As $\boldsymbol{\ell}$ and $\dot{\boldsymbol{\ell}}$ can be evaluated from the motion capture data, and the values from prior studies [10][11] were used for the remaining parameters, $\boldsymbol{F}_{lce}(\boldsymbol{\ell})$ and $\boldsymbol{F}_{vce}(\dot{\boldsymbol{\ell}})$ can be computed using Eqs. (7) and (8). Figs. 2(a) and 2(b) depict the graph diagram of $\boldsymbol{F}_{lce}(\boldsymbol{\ell})$ and $\boldsymbol{F}_{vce}(\dot{\boldsymbol{\ell}})$, respectively. In Fig. 2(a), the dotted and chain lines represent the muscle forces generated from the active and passive properties of the muscle, respectively; the solid line represents the sum of the two muscle forces.

By substituting Eq. (6) into Eq. (2), the following Eq. (12) can be obtained:

$$\boldsymbol{\tau} = \boldsymbol{J}_{\ell}^{T} \boldsymbol{F}_{max} \boldsymbol{F}_{lce}(\boldsymbol{\ell}) \boldsymbol{F}_{vce}(\dot{\boldsymbol{\ell}}) \boldsymbol{a} \tag{12}$$

$$\boldsymbol{\tau} = \boldsymbol{C} \boldsymbol{a}, \tag{13}$$

where $\boldsymbol{C} \in \mathbb{R}^{n \times m}$ is defined as

$$\boldsymbol{C} = \boldsymbol{J}_{\ell}^{T} \boldsymbol{F}_{max} \boldsymbol{F}_{lce}(\boldsymbol{\ell}) \boldsymbol{F}_{vce}(\dot{\boldsymbol{\ell}}). \tag{14}$$

Moreover, $\boldsymbol{C}$ is the matrix of which the row/column is the number of joints and muscles. In this case, we need to increase the number of constraints to determine a unique muscle activity from the computed joint torque, as humans have a redundant drive system with $n < m$. As stated earlier, the muscle activity $\boldsymbol{a}$ was assumed as constant during the time before and after landing. Therefore, $\boldsymbol{a}$ can be obtained by the least-squares method for the following Eq. (15):

$$\arg\min_{\boldsymbol{a}} \frac{1}{2} \left\| \begin{pmatrix} \boldsymbol{\tau}_1 \\ \vdots \\ \boldsymbol{\tau}_T \end{pmatrix} - \begin{pmatrix} \boldsymbol{C}_1 \\ \vdots \\ \boldsymbol{C}_T \end{pmatrix} \boldsymbol{a} \right\|^2, \tag{15}$$

which is subject to the following constraints

$$0 \le a_i \le 1 \ (i = 1, \ldots, m), \tag{16}$$

TABLE I
MUSCLES IN MUSCULOSKELETAL MODEL

ID	Muscle	Wires
1	Psoas Major	9
2	Iliacus	2
3	Sartorius	1
4	Rectus Femoris	1
5	Vastus Lateralis	1
6	Vastus Medialis	1
7	Vastus Intermedius	1
8	Gracilis	1
9	Pectineus	1
10	Adductor Longus	1
11	Adductor Brevis	1
12	Adductor Magnus	3
13	Gluteus Maximus	6
14	Gluteus Medius	3
15	Gluteus Minimus	3
16	Tensor Fasciae Latae	1
17	Piriformis	1
18	Obturatorius Internus	1
19	Gemellus Superior	1
20	Gemellus Inferior	1
21	Quadratus Femoris	1
22	Obturatorius Externus	2
23	Biceps Femoris Short Head	1
24	Biceps Femoris Long Head	1
25	Semitendinosus	1
26	Semimembranosus	1
27	Tibialis Anterior	1
28	Extensor Hallucis Longus	1
29	Extensor Digitorum Longus	3
30	Peroneus Tertius	2
31	Gastrocnemius	2
32	Soleus	2
33	Plantaris	1
34	Popliteus	1
35	Flexor Hallucis Longus	1
36	Flexor Digitorum Longus	1
37	Tibialis Posterior	1
38	Peroneus Longus	1
39	Peroneus Brevis	1

where T represents the number of frames used for analysis. Thus, $\boldsymbol{a}$ representing the agonist and antagonist muscle activities can be obtained.

The number of muscles was $m = 39$ (Table I), and the number of degrees of freedom (DoFs) of the joints were $n = 9$ (3 DoFs each for the hip, knee, and ankle joints). Some muscles are implemented using multiple wires on the musculoskeletal model, and the number of wires of each muscle is shown in the third column of the Table I. In addition, $T = 9$, because the motion was analyzed every 5 ms and 20 ms before and after the IC for a total period of 40 ms. We used MATLAB R2020b as the analysis tool and the lsqlin function for the least-squares method.

C. Adjustment of passive muscle parameters

In addition to the estimation method for the antagonist muscle activity discussed in the previous subsection III-B, the muscle model was adjusted to be suitable for jump landing by altering the parameters representing the passive properties of the muscle. To modify the passive parameters of the muscle, the knee joint torque calculated based on inverse dynamics was compared with that obtained by the proposed method discussed in the previous subsection III-B. The parameters that we modified were the passive muscle strain resulting from the maximum isometric force ε_0^M and the maximum isometric force F_{max}. The muscle becomes harder to stretch when the value of ε_0^M becomes smaller. ε_0^M was investigated for values of 0.60, 0.10, 0.03. Thelen showed that the muscle strain of young adults was 0.60 [11]. Here, we assumed that the muscles are kept stiff in preparation for landing and the muscle strain becomes smaller than 0.60. We also modified F_{max}. The Hill–Stroeve model accounted for the viscoelastic properties of the muscle during its active movement. We investigated F_{max} by multiplying the values shown in [5] by 1.0, 5.0, and 10.0. We assumed that the subject was receiving a large amount of force from the floor when landing, and selected values that were larger than the values shown in [5]. Analysis was performed on the nine models that were created by combining each parameter.

D. Comparison between proposed and conventional methods

The total muscle forces acting in the antagonist relationship of the knee joint obtained using the conventional method [5] were compared with that obtained from the proposed method. As described in subsection III-A, the antagonist muscle activity could not be estimated through the conventional method; therefore, we reviewed whether the antagonist muscle activity could be estimated based on the aforementioned comparison. The parameter values used in this analysis were ε_0^M set to 0.03 and F_{max} multiplied by 10.0, which provided a reasonable correspondence to those obtained earlier (subsection III-C).

IV. MUSCLE ACTIVITY ANALYSIS RESULTS

The following two results were obtained by analyzing the muscle activity.

- Fig. 3 depicts a comparison of the knee joint torque obtained using the inverse dynamics and the proposed method. The black dotted line represents the knee joint torque calculated using the inverse dynamics, whereas the additional three solid lines denote those calculated based on the muscle activities obtained with the proposed method using various passive parameters, i.e., ε_0^M and F_{max}. Figs. 3(a)–3(c) display the torque when ε_0^M is 0.60, 0.10, and 0.03, respectively. In each figure, the values represented by the blue solid line (circular marker), red solid line (asterisk marker), and magenta solid line (square marker) were F_{max} multiplied by a factor of 1.0, 5.0, and 10.0, respectively. The vertical and horizontal axes represent the values of the knee joint torque [Nm] and the number of frames, respectively; the 5th frame corresponds to IC. In this figure, the positive and negative joint torque represent that the joint is flexed and extended, respectively.
- Fig. 4 depicts a comparison of the total muscle forces corresponding to the antagonist relationship of the knee joint obtained using the conventional method [5] and that evaluated using the proposed method. The muscle antagonist relationship related to the knee joint for DVJ motion was set as listed in Table II [14][15]. In Fig. 4, the dotted black and solid red lines represent the

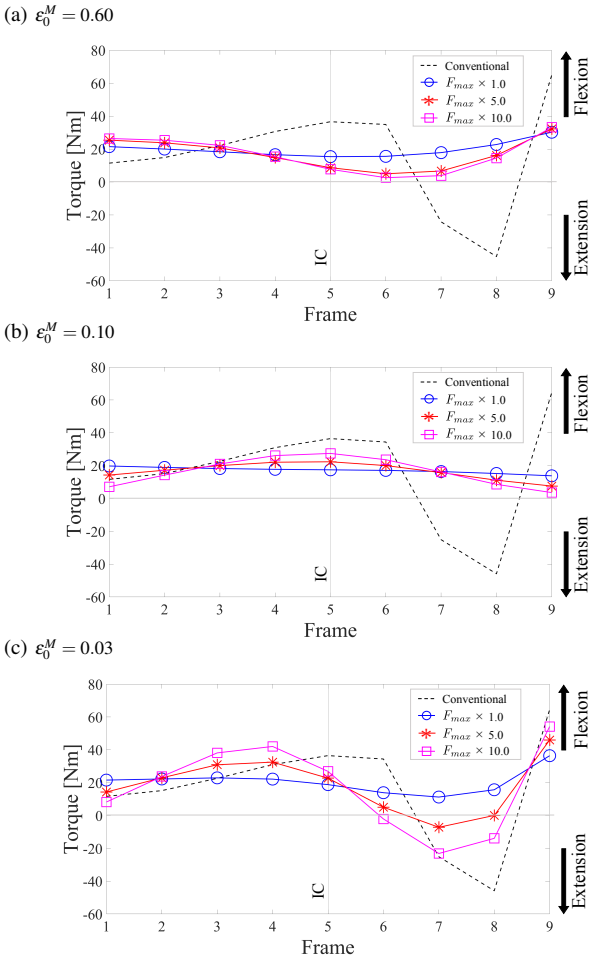

Fig. 3. Comparison of knee joint torque evaluated using inverse dynamics (dotted black line) and that obtained with the proposed method using muscle activities (other three solid lines). The torques calculated using the proposed method varied with the parameter values: (a) $\varepsilon_0^M = 0.60$, (b) $\varepsilon_0^M = 0.10$, and (c) $\varepsilon_0^M = 0.03$. In each figure, the blue (circle markers), red (asterisk markers), and magenta (square markers) lines represent $F_{max} \times 1.0$, $F_{max} \times 5.0$, and $F_{max} \times 10.0$, respectively. The vertical and horizontal axes represent the joint torque value and number of frames, respectively; the time between frames was 5 ms, and the 5th frame corresponds to IC timing. A positive and negative joint torque indicate that the joint is flexed and extended, respectively.

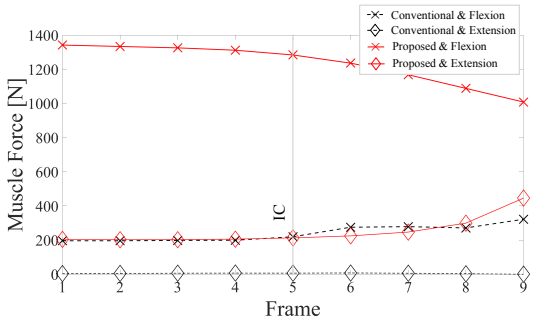

Fig. 4. Comparison of the sum of muscle forces related to knee joint antagonist relationship (Flexion & Extension) calculated from inverse dynamics (dotted black line) and from the muscle activity obtained using the proposed method (solid red line). Flexion and extension motions are represented using "x" and diamond-shaped markers, respectively. The vertical and horizontal axes represent the muscle force value and the number of frames, respectively; the time between the frames is 5 ms, and the 5th frame corresponds to IC timing.

total muscle forces obtained using the conventional and proposed method, respectively. Flexion and extension motions are represented using "x" and diamond-shaped markers, respectively. In addition, the vertical and horizontal axes depict the total muscle force [N] and the number of frames, respectively; the 5th frame corresponds to IC.

V. Discussion

Based on the abovementioned results, the following two considerations were obtained.

- From Fig. 3, the knee joint torque decreased immediately after landing as the value of ε_0^M decreased and that of F_{max} increased. Moreover, ε_0^M represented the elongation rate of the tendon; a small value maintained the muscle rigidity owing to the posture preparation for landing. A prior study described the muscle strain during passive pulling of the gastrocnemius muscle of a rabbit [16]. As the strain evaluated in the aforementioned study was 0.04 for approximately 30 ms after the start of the pull, the value of $\varepsilon_0^M = 0.03$ can be considered appropriate. For F_{max}, the original value from the Hill–Stroeve model was used. Although the Hill–Stroeve model accounts for the viscoelastic properties of the muscle during its active movement, the proposed model focused on the passive properties of the muscle. Therefore, the results of Fig. 3 indicate that the passive properties of the muscle may possess a tolerance of F_{max} which is 10.0 times that of the active property. Thus, the passive parameters of the muscle were adjusted to ensure suitability of the developed model under heavy load conditions of DVJ landing.
- Based on the results presented in Fig. 4, the muscle force obtained from the proposed method was generally larger than that obtained using the conventional method. Presumably, the deviation between these two muscle forces was caused by the activities of the antagonist muscle, which can be estimated by the algorithm for muscle activity estimation developed in this study. Moreover, the variation in the moment arm of each muscle may have generated a much larger agonist muscle force than the antagonist muscle force obtained using the proposed method. In this study, we adjusted the passive muscle parameters to estimate the muscle forces based on the computed joint torque. Therefore, the agonist muscle force output was larger than its actual

TABLE II
Relationship of Antagonist Muscle with Knee Joint During Motion [14][15]

Motion	Muscle	Motion	Muscle
Flexion	Sartorius	Extension	Rectus Femoris
	Gracilis		Vastus Lateralis
	Biceps Femoris Short Head		Vastus Medialis
	Biceps Femoris Long Head		Vastus Intermedius
	Semitendinosus		
	Semimembranosus		
	Gastrocnemius		
	Plantaris		
	Popliteus		

value, because the moment arm of the agonist muscles was smaller than that of the antagonist muscles. As a future research direction, the proposed method should be validated with muscle activities measured using an EMG not used in this study.

- The adjustment of the passive muscle parameters revealed the muscle behavior under heavy load environment of landing. We applied the same parameters to all lower limb muscles in this study. Adjusting these muscle parameters for each muscle will help identify muscles that are subjected to exceptionally large loads during landing. Training these load-bearing muscles and changing the motion so as to avoid subjecting these muscles to large loads on the knee joint would be helpful in preventing ACL injuries.

VI. Conclusion

This study investigated a passive muscle mechanical model for heavy load environments such as jump landing to estimate the activity of antagonist muscles. The model was applied to the Hill's equation for estimating the muscle activity during DVJ. The knee joint torque evaluated using inverse dynamics was compared with that obtained from the proposed method, and the values of the passive muscle strain resulting from the maximum isometric force ε_0^M, including the value of the maximum isometric force F_{max}, were varied in the proposed method to reconstruct the knee joint torque. Based on these results, we developed a passive muscle mechanical model that was suitable for representing the landing by decreasing the value of ε_0^M and increasing that of F_{max}. The proposed model was used with ε_0^M set to 0.03 and F_{max} multiplied by 10.0. Subsequently, the muscle force pertaining to the antagonist relationship of the knee joint was determined and compared with that obtained using the conventional method [5]. Consequently, the muscle force obtained by the proposed method exhibited a larger value than that resulting from the conventional method. This study developed a method to identify the level of preparation, namely, co-contraction, before contact in DVJ. This provides useful information to analyze the risk of muscle/tendon/ligament injuries, including ACL injuries. The preparation for contact is a tacit skill in athletes and is difficult to explain or train for. The results of this study provide a possible approach to quantify and visualize this tacit skill in athletes.

References

[1] B. P. Boden, G. S. Dean, J. A. Feagin Jr., and W. E. Garrett Jr., Mechanisms of anterior cruciate ligament injury, Orthopedics, vol. 23, no. 6, pp. 573–578, 2000.

[2] T. E. Hewett, G. D. Myer, K. R. Ford, R. S. Heidt Jr., A. J. Colosimo, S. G. McLean, A. J. van den Bogert, M. V. Paterno, and P. Succop, Biomechanical measures of neuromuscular control and valgus loading of the knee predict anterior cruciate ligament injury risk in female athletes. Am. J. Sports Med, Vol. 33, No. 4, pp. 492–501, 2005.

[3] F. T. Sheehan, W. H. Sipprell III, and B. P. Boden, Dynamic sagittal plane trunk control during anterior cruciate ligament injury, Am. J. Sports Med., vol. 40, no. 5, pp. 1068–1074, 2012.

[4] A. M. Smith, The coactivation of antagonist muscles, Can. J. Physiol. Pharmacol., vol. 59, no. 7, pp. 733–747, 1981.

[5] Y. Nakamura, K. Yamane, Y. Fujita, and I. Suzuki, Somatosensory computation for man-machine interface from motion-capture data and musculoskeletal human model, IEEE Trans. Robo., vol. 21, no. 1, pp. 58–66, 2005.

[6] H. Koga, A. Nakamae, Y. Shima, J. Iwasa, G. Myklebust, L. Engebretsen, R. Bahr, and T. Krosshaug, Mechanisms for noncontact anterior cruciate ligament injuries: Knee joint kinematics in 10 injury situations from female team handball and basketball, Am. J. Sports Med, vol. 38, no. 11, pp.2218–2225, 2010.

[7] D. M. Corden, O. C. J. Lippold, K. Buchanan, and C. Norrington, Long-latency component of the stretch reflex in human muscle is not mediates by intramuscular stretch receptors, J. Neurophysiol., vol. 84, no. 1, pp. 184–188, 2000.

[8] H. Suzuki, Y. Ikegami, E. Uchiyama, K. Yamamoto, A. Yamada, Y. Nakamura, Y. Mizutani, K. Kawaguchi, and S. Taketomi, Anterior cruciate ligament injury risk assessment study based on biomechanical analysis of drop vertical jump (in Japanese), 25th Robotics Symposia, pp. 173–178, 2020.

[9] A. V. Hill, The heat of shortening and the dynamic constants of muscle, Proc. R. Soc. B, vol. 126, no. 843, pp. 136–195, 1938.

[10] S. Stroeve, Impedance characteristic of a neuromusculoskeletal model of the human arm I. Posture control, Biol. Cybern., vol. 81, no. 5-6, pp. 475–494, 1999.

[11] D. G. Thelen, Adjustment of muscle mechanics model parameters to simulate dynamic contractions in older adults, J. Biomech. Eng., vol. 125, no. 1, pp. 70–77, 2003.

[12] T. Horikawa, Y. Ikegami, H. Obara, A. Yamada, K. Kawaguchi, S. Taketomi, and Y. Nakamura, Aquisition of Large Scale Jump Motion Data Using Video Motion Capture System for Risk Analysis of Athletes' Knee Injury (in Japanese), 24th Robotics Symposia, pp. 346–349, 2019.

[13] E. Uchiyama, H. Suzuki, Y. Ikegami, Y. Nakamura, S. Taketomi, K. Kawaguchi, Y. Mizutani, and T. Doi. Muscles Cooperation Analysis Using Akaike Information Criteria for Anterior Cruciate Ligament Injury Prevention, IEEE EMBC, pp. 4799–4802, 2020.

[14] M. Schünke, E. Schulte, U. Schumacher, M. Voll, and K. Wesker, General anatomy and Movement System Prometheus Anatomy Atlas [Translated by T. Sakai and J. Matsumura], 3rd ed., Igaku-Shoin, 2017.

[15] H. J. Hislop, D. Avers, and M. Brown, Daniels and Worthingham's muscle testing: Techniques of manual examination and performance testing [Translated by N. Tsuyama and K. Nakamura], 9th ed., Kyodo Medical Book Publisher, 2014.

[16] M. Hayashibe, P. Poignet, D. Guiraud, and H. E. Makssoud, Nonlinear identification of skeletal muscle dynamics with Sigma-Point Kalman Filter for model-based FES, IEEE ICRA, pp. 2049–2054, 2008.